Journal of Sound and Vibration (2000) **238**(2), 215–231
doi:10.1006/jsvi.2000.3081, available online at http://www.idealibrary.com on IDEAL®

NEURO-ADAPTIVE VIBRATION CONTROL OF COMPOSITE BEAMS SUBJECT TO SUDDEN DELAMINATION

S.-H. Youn†, J.-H. Han and I. Lee

Department of Aerospace Engineering, Korea Advanced Institute of Science and Technology, 373-1, *Kusong-dong, Yusong-gu, Taejon, South Korea. E-mail: inlee@asdl.kaist.ac.kr*

(*Received* 18 *December* 1999, *and in final form* 4 *May* 2000)

Experimental studies on the adaptive vibration control of composite beams with a piezoelectric actuator have been performed using a neural network controller. We experimentally investigated the variations in natural frequencies and actuation characteristics of the composite specimens according to delaminations in the bonding layer. Numerical simulation has been performed for adaptive vibration controls of the composite specimens with delaminated piezoelectric actuator using the neuro-controller. A digital signal processor (DSP)-based hardware for the real-time adaptive vibration control experiment was prepared. Using the neuro-controller, the adaptive vibration control experiment has been performed. The vibration control results show that the present neuro-controller has good performance and robustness with respect to the system parameter variations.

1. INTRODUCTION

In the past several decades, composite materials have been increasingly used in many advanced structural applications such as modern aircraft structures in order to reduce structural weight and to increase performances. However, these lightweight composite structures are prone to excessive vibration, which might degrade system performances and sometimes yield structural failure. Therefore, there have been active research interests on the structural vibration suppression using passive and/or active control methods. Among several efforts, active vibration control using smart materials has been the recent interest [1]. Especially, piezoelectric sensors and actuators have attracted attention in the active vibration control area because of several promising properties such that they have distributed nature, wide frequency-band characteristics, and many others [2–5]. To date, time-invariant control algorithms such as Lyapunov algorithms in references [2, 3], and optimal control algorithms in references [4, 5] have been usually used in the active vibration control of smart structures.

In the real service life, however, all structures are subjected to repeated loads, low- and high-velocity impacts, and thermal stresses. These environmental loads can sometimes cause local structural failure, and hence result in changes in dynamic characteristics of

†Present address: Rocket Structures/Materials Department, Korea Aerospace Research Institute, Yusong P.O. Box 113, Taejon, South Korea.

0022-460X/00/470215 + 17 $35.00/0

structures [6]. In addition, structural systems having time-varying characteristics without permanent structural damages can be easily found. For example, the dynamic characteristics of a spacecraft can vary due to severe temperature variations during its attitude changes. When dynamic characteristics of structures are varying, vibration control using conventional linear time-invariant control algorithm may result in inefficient vibration suppression, or even amplify structural vibration until structural failure occurs. Among several causes for system variations, delamination in the piezoelectric bonding layer is the main interest in this study. Kim and Jones [7] studied variations of natural frequencies of beams with delamination of various sizes in piezoelectric bonding layer. They showed that the delamination leads to decrease in natural frequencies. In the present paper, these parameter variations have been measured by using the experimental modal testing. In this study, the adaptive feedback control methodologies using neural networks are investigated for the active vibration suppression of composite structures subject to sudden delamination.

Neural networks have been successfully applied in several engineering areas such as pattern recognition and optimization problems, because neural networks have excellent interpolation capabilities so that the mapping between inputs and outputs of non-linear systems can be effectively obtained [8]. Due to these good interpolation capabilities, successful system identifications in a noisy environment can be achieved using neural networks. Besides these classical applications, there have been increasing efforts to make use of artificial neural networks for robust adaptive control in several engineering fields such as high-performance aircraft/missile control and robot trajectory planning and so on [9].

The research on neural network-based vibration controls can be divided into two categories: feedforward and feedback control methods. Feedforward controls generally utilize a reference signal, which is correlated with the impending primary disturbance, for the derivation of control input. Snyder and Tanaka [10] developed a neural network/algorithm, which can be regarded as a non-linear generalization of transversal filter/filtered-x LMS algorithm, for non-linear feedforward-control systems. They also conducted experimental works to demonstrate the utility of the algorithm, showing that it is well suited for a non-linear control problem [11]. On the other hand, feedback controls generally rely on the error signals to construct control signals for the non-availability of the reference signals. Narendra and Parthasarathy [12] investigated several methods about identification and control of dynamical systems using neural networks. KrishnaKumar and Montgomery [13] performed adaptive control of large flexible structures using a neuro-controller. They used a clamped-free beam specimen as an experimental model and applied both off-line neuro-controller training and on-line fast-learning with error critics for the experimental study. Rao *et al.* [14] presented numerical studies of adaptive controls for vibration suppression of smart structures with shape memory alloy (SMA) actuators. Chandrashekhara and Smyser [15] developed a numerical dynamic model for the active vibration control of laminated doubly curved shells. In their study, a neural network controller was designed and trained off-line to emulate the performance of linear quadratic Gaussian with loop transfer recovery (LQG/LTR) controller. Vibration controls using neural networks with Marquardt algorithms and optimal neural design methodologies using the Taguchi method have also been studied [16, 17].

Even though many relevant works have been accomplished, experimental studies on real-time adaptive vibration control are still rare. Since one of the key features of smart structures is adaptability, we are very interested in the implementation of adaptive control that has sufficient robustness and generality.

In summary, neuro-adaptive feedback control algorithms have been applied to suppress the vibrations of composite structures subject to sudden delamination in the present study.

In what follows, we first experimentally investigate the variations of dynamic characteristics of composite structures due to delaminations. In section 3, the basic learning method of neural networks is introduced. In section 4, the adaptive system identifier and controller model are proposed, and the performance of the model is examined by numerical simulation. Finally, the real-time implementation of the adaptive controller was performed using a digital signal processor (DSP). The present adaptive control method was proved to be robust with local structural failure. Note that, in this paper, only delamination effect has been considered as the origin of the system variations, but there is every reason that the present method can also be used in other structural systems with diverse non-linear and/or time-varying characteristics.

2. DYNAMIC CHARACTERISTICS OF COMPOSITE BEAMS WITH DELAMINATION

The equation of motion of a structural system with a piezoelectric actuator in modal co-ordinate can be written as follows:

$$\ddot{\eta}_r + 2\zeta_r \omega_{nr} \dot{\eta}_r + \omega_{nr}^2 \eta_r = f_r V \quad (r = 1, 2, \ldots, \infty), \tag{1}$$

where η_r, $\dot{\eta}_r$ and $\ddot{\eta}_r$ represent modal displacement, velocity, and acceleration, respectively; ω_{nr} and ζ_r are natural frequency and damping ratio of the rth mode; f_r and V represent modal actuation force due to unit applied voltage and control voltage respectively.

Distributed piezoelectric actuator has several advantages over conventional actuators, but it serves not only as an active component but also as a passive load-bearing element. Therefore, it is difficult to estimate the characteristics of piezoelectric actuation force f_r, which is affected by the size and location of the actuator, bonding layer properties, mode shapes, and the material properties of piezoelectric actuator itself. In this analysis, variations of natural frequencies and modal control forces of composite specimens with a delaminated piezoelectric actuator are experimentally investigated.

Composite specimens were prepared from unidirectional graphite/epoxy prepreg tapes. the prepreg tapes were laid up into a laminate with appropriate layer angles. Layered prepreg were cured in the panel autoclave at KAIST under the curing cycle recommended by the manufacturer. A piezoelectric actuator was bonded on the surface of laminated composites using epoxy adhesive. In order to prepare delaminated specimens, a very thin Teflon film was inserted in the desired location. Figure 1 and Table 1 show configurations and dimensions of the specimens used in this experiment. In order to investigate modal control force, natural frequencies and mass-normalized mode shapes were first obtained from the conventional modal testing by using a laser displacement sensor and an impact hammer. The normalized mode shapes at a certain point can be obtained by coinciding the sensing and impacting points. After obtaining dynamic characteristics of the specimen, the

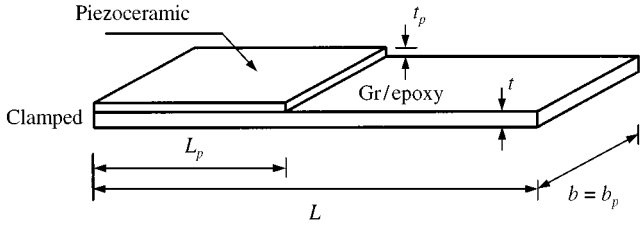

Figure 1. Geometry of the composite beam with a delaminated piezoceramic actuator.

TABLE 1

Dimensions and configurations of the composite beams with a delaminated piezoceramic actuator

Specimen no.	Stacking sequence (Gr/epoxy)	Dimensions of host structure $L \times b \times t$ (mm^3)	Dimensions of piezoceramic $L_p \times b_p \times t_p$ (mm^3)	Delamination size (mm)	Thickness of adhesive (mm)
1	$[0/\pm 45/90]_s$	$220 \times 20 \times 0{\cdot}835$	$50 \times 20 \times 0{\cdot}4$	0	0·04
2	$[0/\pm 45/90]_s$	$220 \times 20 \times 0{\cdot}835$	$50 \times 20 \times 0{\cdot}4$	12·5	0·04
3	$[0/\pm 45/90]_s$	$220 \times 20 \times 0{\cdot}835$	$50 \times 20 \times 0{\cdot}4$	25·0	0·04
4	$[0/\pm 45/90]_s$	$220 \times 20 \times 0{\cdot}835$	$50 \times 20 \times 0{\cdot}4$	37·5	0·04

Note: Displacement sensor location for control: 20 mm from the clamped boundary.

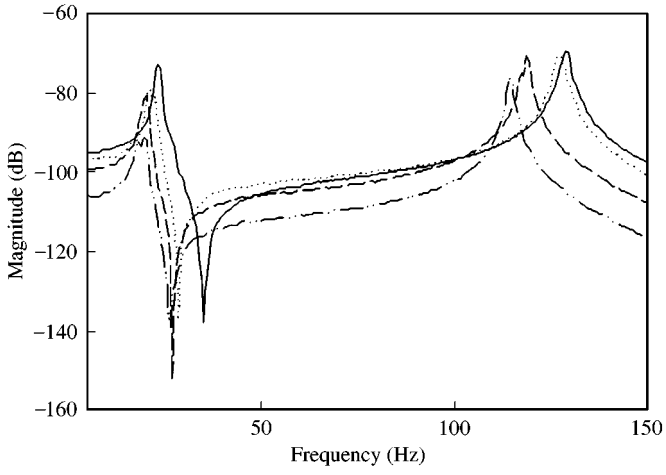

Figure 2. Frequency response functions for the composite specimen with a delaminated piezoceramic actuator. ——, 0% delamination; --------, 25% delamination; — —, 50% delamination; — ··, 75% delamination.

transfer function between the input voltage to the piezoelectric actuator and deflections obtained by the laser sensor has been measured. The actuation characteristics can be obtained from this transfer function. Further details can be found in reference [18].

Figure 2 shows the frequency response functions of the specimens with a delamination of various sizes. Variations of the first and second natural frequencies and modal control forces are summarized in Table 2. It is clearly shown that natural frequencies and modal control forces decrease as the length of delamination increases. Specifically, the first modal actuation force of the specimen with 75% delamination reduces to one-seventh of that of the normal specimen. The measured modal control force of the second mode of 25% delaminated specimen is a little higher than that of the normal specimen. The reason is that the curvature of the second mode shape changes at the bonding location of piezoelectric actuator. Therefore, there is a cancellation of piezoelectric actuation for the normal specimen.

As investigated above, natural frequencies and modal control forces vary significantly when delamination of piezoelectric actuator occurs. Therefore, an adaptive control algorithm is essential to control such systems.

TABLE 2

First and second frequencies, and modal control forces for Gr/Epoxy $[0/\pm 45/90]_s$ *composite beams with a delaminated piezoceramic actuator*

Specimen no.	Delamination size (mm)	First frequency (Hz)	First modal control force (s^{-2}/V)	Second frequency (Hz)	Second modal control force (s^{-2}/V)
1 (Experiment)	0 (0%)	23·739	0·006977	128·697	0·02957
2 (Experiment)	12·5 (25%)	21·843	0·005287	127·384	0·03113
3 (Experiment)	25 (50%)	20·152	0·002333	118·325	0·01598
4 (Experiment)	37·5 (75%)	19·284	0·001001	114·547	0·007937

3. BASICS FOR NEURAL NETWORKS

Neural network is a mathematical model, which is artificially embodied by imitating recognition or knowledge-acquiring process of human beings [19]. A neural network consists of neurons, weights and biases. A basic multi-layer neural network structure is shown in Figure 3. Learning is defined as a process that tunes weights and biases so as to obtain the desired output values of the neural network. When learning procedure proceeds using known input/output patterns, it is called supervised learning. Among several learning algorithms, error back-propagation learning rule is most widely used and this algorithm is applied in this study. The fundamental idea of the algorithm is to adjust weights and biases of neural network so that the sum of squared error of outputs is to be minimized.

The neural network used in this study consists of three layers; one input layer, one hidden layer, and one output layer. In what follows, the subscripts i, j, and k denote the respective input, hidden, and output layer properties to prevent any confusion. Tangent sigmoid transfer function was used for the hidden layer, and linear transfer function was used for the output layer. The output error $E(\mathbf{w}, \mathbf{b})$ to be minimized by adjusting weights and biases is defined as

$$E = \frac{1}{2}\sum_k (d_k - O_k)^2, \tag{2}$$

where d_k and O_k represent the desired output and the output of neural network respectively. Using gradient descent procedure, variation of weights connecting hidden and output layers is obtained as follows:

$$\Delta w_{kj} = -\eta(\partial E/\partial w_{kj}), \tag{3}$$

where η represents the step size and is called learning rate. The changes of the error with respect to weight variations can be written as

$$\partial E/\partial w_{kj} = -(d_k - O_k) f_k'(net_k) O_j = -\delta_k O_j, \tag{4}$$

where O_j, f_k, and $(\,)'$ represent output values of the hidden layer, linear transfer function of the output layer, and differentiation operator respectively. net_k is defined as $\sum_j w_{kj} O_j$, and

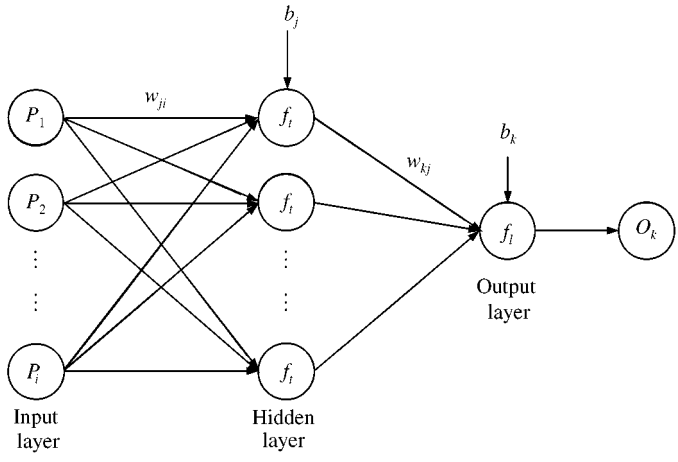

Figure 3. A layered neural network.

$\delta_k = (d_k - O_k)\, f_k'(net_k)$ stands for the kth layer's error gradient. δ_k is usually called delta function. Therefore, the variations of weights can be written in a compact form as follows:

$$\Delta w_{kj} = \eta \delta_k O_j. \tag{5}$$

Using similar procedures, the variations of the kth layer's biases can be obtained as follows:

$$\Delta b_k = \eta (d_k - O_k). \tag{6}$$

On the other hand, the desired output values of the hidden layer are not given in an explicit way. Therefore, the weights and biases of the hidden layer should be calculated by using chain rules. The variations of weights between input and hidden layers can be calculated as follows:

$$\Delta w_{ji} = -\eta(\partial E/\partial w_{ji}) = -\eta(\partial E/\partial O_j)(\partial O_j/\partial w_{ji}), \tag{7}$$

where

$$\begin{aligned} \partial E/\partial O_j &= \sum_k (\partial E/\partial O_k)(\partial O_k/\partial O_j) \\ &= -\sum_k (d_k - O_k)\, f_k'(net_k)\, w_{kj} = -\sum_k \delta_k w_{kj}. \end{aligned} \tag{8}$$

Using Equation (8), Equation (7) can be written as follows:

$$\partial E/\partial w_{ji} = -\left(\sum_k \delta_k w_{kj}\right) f_j'(net_j)\, P_i = -\delta_j P_i, \tag{9}$$

where f_j and P_i represent transfer function of the hidden layer and input values to the neural network respectively. net_j is defined as $\sum_i w_{ji} P_i$, and δ_j stands for the delta function of the jth layer and can be written as

$$\delta_j = \left(\sum_k \delta_k w_{kj}\right) f_j'(net_j). \tag{10}$$

Therefore, the variations of weights between input and hidden layers can be written in a compact form as follows:

$$\Delta w_{ji} = \eta \delta_j P_i. \tag{11}$$

Using similar procedures, the variations of the jth layer's biases can be obtained as follows:

$$\Delta b_j = \eta \left(\sum_k \delta_k w_{kj} \right). \tag{12}$$

When the error back-propagation learning algorithm is applied, both the momentum method and the adaptive learning rate method are often used in order to improve convergence characteristics and the convergent speed [20, 21].

4. ADAPTIVE VIBRATION CONTROL USING NEURO-CONTROLLER

Among several control methodologies, the indirect model reference adaptive controller has been used in this study. The control system consists of the neuro-identification model and the neuro-controller, and the overall architecture of the controller is shown in Figure 4.

The role of the neural network model (identifier) for the plant is to obtain mathematical representation of the real plant. This procedure is called forward modelling. The neural network model is located in parallel with the plant as shown in Figure 5. The weights and biases of the neural network model are adjusted so that the output of the neural network model should be the same as that of the plant. The input values of the neural network model are the present and previous plant inputs and outputs. In other words, the output value of neural network model y_m is calculated by using time sequences of the plant input u and plant output y_p as follows:

$$y_m(t+1) = f(y_p(t), \ \ldots \ , y_p(t-n); u(t), \ \ldots \ , u(t-m)). \tag{13}$$

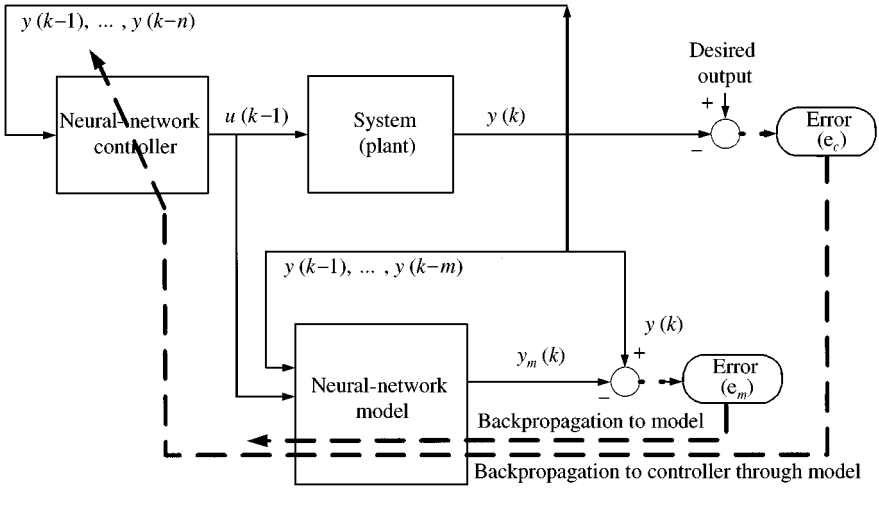

Figure 4. Overall architecture for neuro-controller with neural-network model.

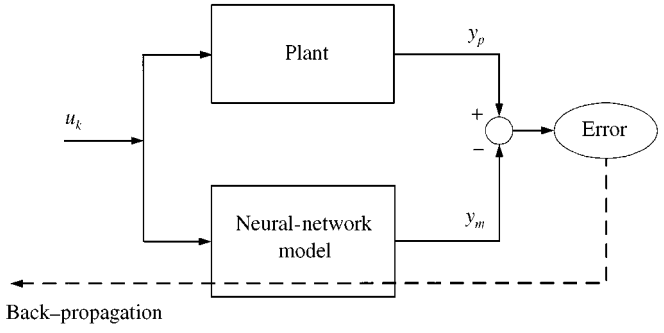

Figure 5. Forward modelling using neural network.

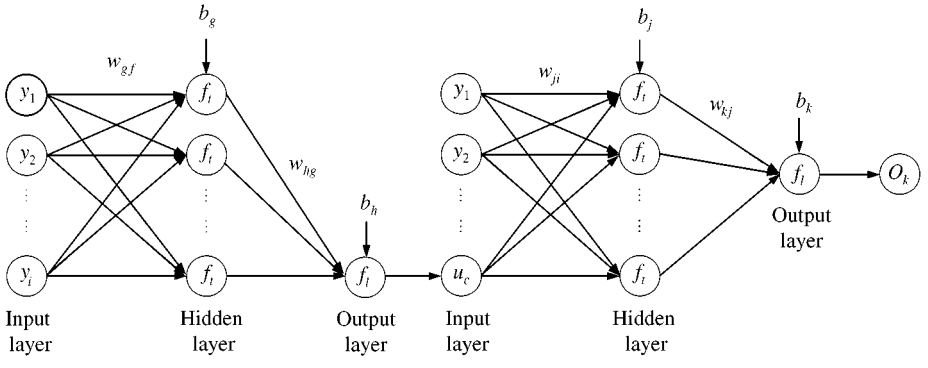

Figure 6. Connection of neural-network model and neuro-controller.

After completing the forward modelling, the tuning for weights and biases of the neuro-controller is performed by the error-back-propagation learning algorithm. Because the desired output value of the neuro-controller is not given in advance, this value should be calculated by the error-back propagation through the neural network plant model, as shown in Figure 6. In this step, the desired output value of the plant is set to zero because the purpose of the control is to suppress vibrations. When adjusting the weights and biases of the neuro-controller, those of the neural network model are not changed. The output of the neuro-controller, u_c is calculated by using time sequences of the plant output, y_p as follows:

$$u_c(t) = f(y_p(t-1), y_p(t-2), \ldots, y_p(t-n)). \tag{14}$$

The numerical simulation for the adaptive vibration control has been performed by using MATLAB and SIMULINK [22]. The experimental results in section 2 give the numerical model of the plant. The neuro-controller has 10 and 20 neurons for the input and hidden layers, respectively, and one neuron for the output layer. The output value of the neuro-controller is used as both the control force of the plant and the 10th input of neural network model. Here, the control force is the applied voltage to the piezo ceramic actuator. The 10 previous output values of plant are used as input of neuro-controller. The neural network model has 10 neurons for both input and hidden layers and one neuron for the output layer. Nine previous output values of plant and output of neuro-controller are used as the input values of the neural network model.

In the numerical investigation, the sampling frequency 1 kHz has been used. The plant output is given as the displacement signal, which is measured 20 mm apart from the clamped boundary. External disturbances given in equation (15) are also applied to the piezoceramic actuator.

$$u = 40[square(\omega_1 t) + square(\omega_2 t)] \quad \text{(V)}, \tag{15}$$

where ω_1 and ω_2 are the first and second natural frequencies of the specimen, respectively; $square(\omega t)$ is the 1 V peak-to-peak square wave signal with the angular frequency of ω. Figure 7 shows the control results when the external disturbance is applied during the first 1 s and the control action begins at 1 s. The displacement signal is shown in Figure 7(a) when 75% delamination occurs abruptly at 1.1 s. It is found that the present adaptive algorithm is adequate for vibration control when the abrupt delamination occurs in piezoelectric bonding layer. Figure 7(b) shows the control results when delamination occurs successively: from 0 to 25% at 1.07 s, to 50% at 1.14 s, and to 75% at 1.21 s. Good control

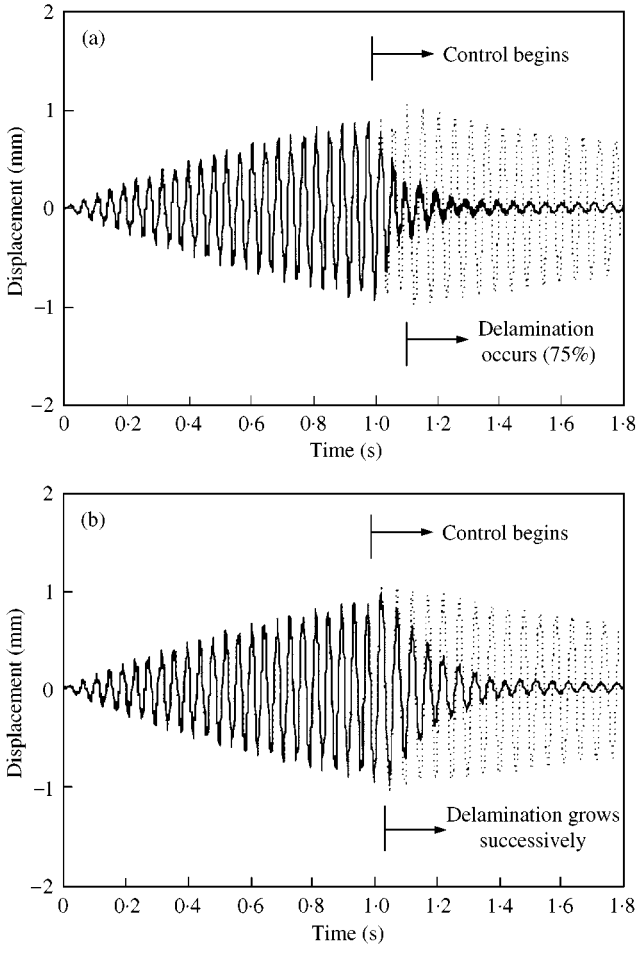

Figure 7. Transient vibration control for the Gr/epoxy $[0/\pm 45/90]_s$ composite specimen: (a) Adaptive vibration control result when 75% delamination occurs at 1·1 s; (b) Adaptive vibration control result when the length of delamination grows successively. —, controlled; ·····, uncontrolled.

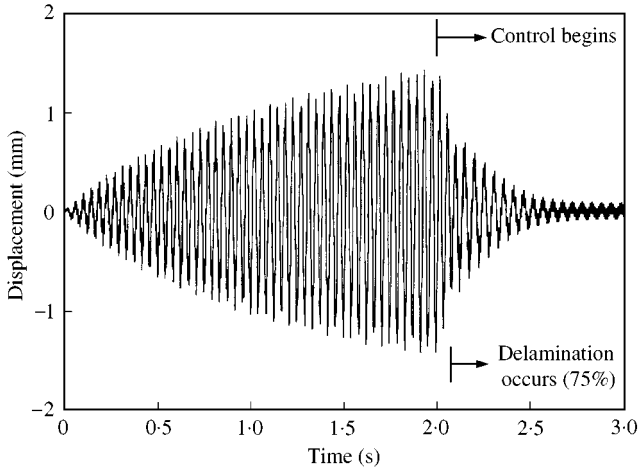

Figure 8. Adaptive vibration control result for the Gr/epoxy $[0/\pm 45/90]_s$ composite beam when the 75% delamination occurs at 2·1 s under persistent disturbance.

result is observed when the successive delamination occurs in piezoelectric bonding layer during control.

Figure 8 shows the control results with persistent external disturbances. The control action begins at 2 s. The 75% delamination occurs suddenly at 0.1 s after the application of the control. It is observed that the present control system gives a good result even though the disturbances are applied continuously.

From the above simulation results, the robustness of the present control system with respect to the system parameter variations has been verified. Note that in the numerical investigation, the performance of the controller is proved to be excellent even though very abrupt changes of the plant are considered.

5. REAL-TIME ADAPTIVE VIBRATION-CONTROL EXPERIMENT

In this section, the real-time adaptive vibration-control experiment has been performed. In the experiment, tuning procedure for the neuro-controller and the neural-network model should be accomplished in real time. Therefore, the number of neurons and the number of maximum iteration are a little reduced in spite of sacrifice of control effectiveness. In addition, tip masses are attached to the beam specimen in order to lower natural frequencies of composite specimens. Figure 9 and Table 3 show the configurations of composite specimens used in the experiment. Normal and 50% delaminated specimens, on which 30 g tip masses are attached, are used. Figure 10 shows the variations of the frequency response due to the delamination. The first frequency and the first modal actuation force of each specimen are summarized in Table 4. It is observed that the 50% delaminated specimen has 30% decreased first natural frequency and 50% decreased first modal actuation force compared with those of the normal specimen.

Numbers of neurons for input and hidden layers of the neuro-controller are 10 and 8 respectively. The sampling frequency in real-time experiment is 100 Hz and the displacement sensor is located 80 mm apart from the clamped boundary for the control. Other parameters in the experiment are the same as those in section 4. The overall real-time experimental set-up for the neuro-adaptive vibration control is shown in Figure 11. The

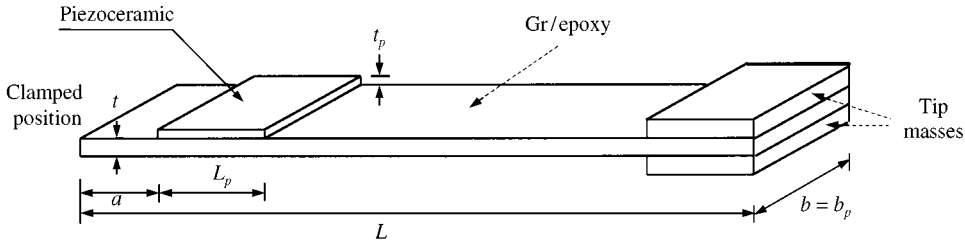

Figure 9. Geometry of the Gr/epoxy $[0/90]_s$ composite beam with a delaminated piezoactuator and tip masses.

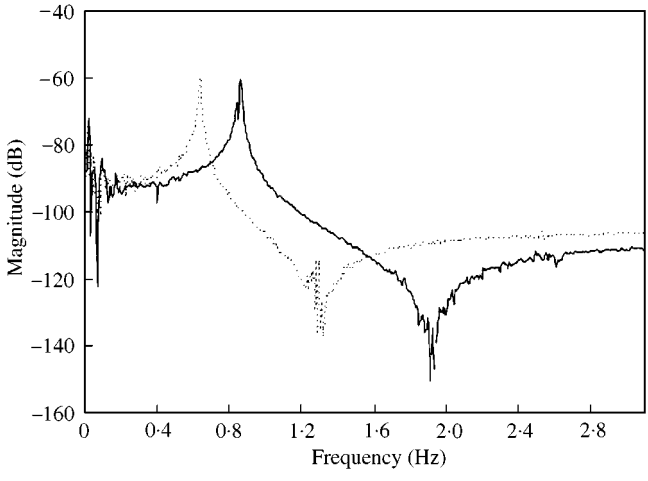

Figure 10. Frequency response functions for Gr/epoxy $[0/90]_s$ composite beams with a delaminated piezoactuator and tip masses ——, 0% Delaminated specimen; ·····, 50% Delaminated specimen.

TABLE 3

Dimensions and configurations of the composite beams with a delaminated piezoceramic actuator and tip masses

Specimen no.	Stacking sequence (Gr/epoxy)	Dimensions of host structure $L \times b \times t$ (mm^3)	Dimensions of piezoceramic $L_p \times b_p \times t_p$ (mm^3)	Actuator location a (mm)	Delamination size (mm)	Thickness of adhesive (mm)
5	$[0/90]_s$	$300 \times 20 \times 0{\cdot}425$	$50 \times 20 \times 0{\cdot}2$	20	0	0·04
6	$[0/90]_s$	$300 \times 20 \times 0{\cdot}425$	$50 \times 20 \times 0{\cdot}2$	20	25	0·04

Note: Displacement sensor location for control: 80 mm from the clamped boundary.

control algorithm is implemented using a DSP board (dSPACE DS1102). DS1102 uses TMS320C DSP chip of Texas Instrument as a base component, and is equipped with 4 A/D and 4 D/A converters. The external disturbance is generated from the source channel of the FFT analyzer, and the laser displacement sensor is used to obtain displacement signal.

Figure 12 shows the changes of the frequency response functions of each specimen due to the application of the control. These frequency responses were obtained by applying

TABLE 4

First frequency and modal control force of Gr/Epoxy $[0/90]_s$ *composite beams with a delaminated piezoceramic and tip masses*

Specimen no.	Delamination size (mm) (%)	First frequency (Hz)	First modal control force (s^{-2}/V)
5 (Experiment)	0 (0%)	0·859	0·0002670
6 (Experiment)	25 (50%)	0·625	0·0001384

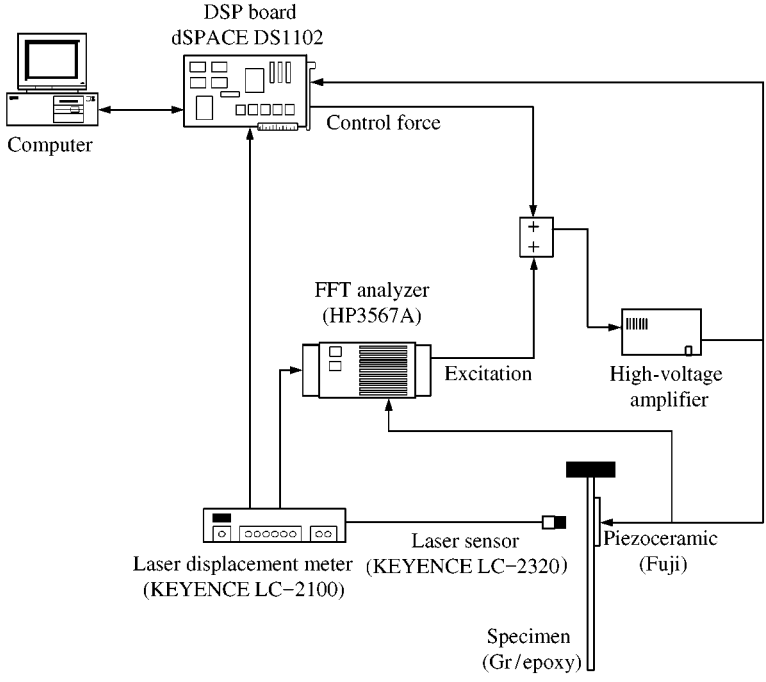

Figure 11. Experimental set-up for the real-time vibration control using neuro-controller.

random external disturbance (maximum magnitude: 8 V, frequency range: 0–3.16 Hz). Significant reductions of the vibrational level of the first mode were observed for both the specimens. In this experiment, the system parameter variations were not considered. The reason why it is more effective to control the vibration of the 50% delaminated specimen is that the first frequency of this specimen is lower than that of the normal specimen. Therefore, it is possible for neural network parameters to be adjusted more delicately for the 50% delaminated specimen.

Figure 13 shows the control results when the delamination occurs suddenly during control. It is difficult to make delamination abruptly during the experiment. Therefore, in the course of the control of the normal specimen, the weights and biases of the neuro-controller and neural-network model were saved. Then the specimen was replaced with the 50% delaminated specimen and the saved weights and biases of neuro-controller and neural-network model were used as the initial values of weights and biases for the next

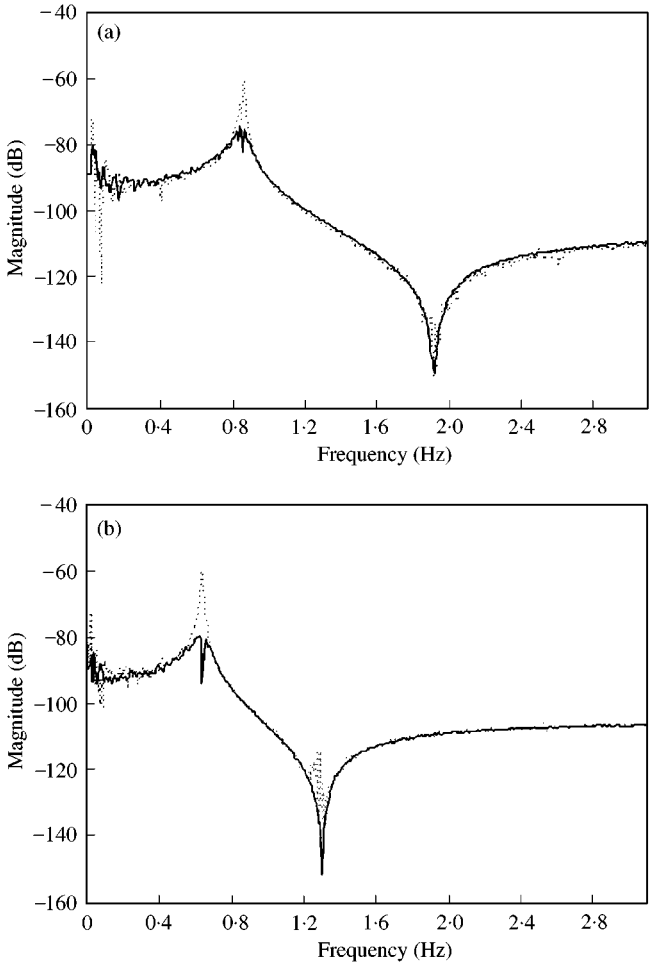

Figure 12. Vibration control results for the Gr/epoxy $[0/90]_s$ composite specimen. (a) 0% delaminated specimen with tip masses, (b) 50% delaminated specimen with tip masses. —, controlled; ····, uncontrolled.

control experiment. External disturbances were applied continuously as

$$u = 5 \times \sin(\omega_1 t) \quad \text{(V)}. \tag{16}$$

Figure 13(a) shows the control result when the control begins at 10 s for the normal specimen. On beginning control, learning of neuro-controller and neural-network model started and weights and biases of neuro-controller and neural-network model were saved for the next initial values at 35 s. The magnitude of the sensor signal was reduced to about 5% of the uncontrolled magnitude. Figure 13(b) shows the control result for the 50% delaminated specimen. In Figure 13(b), the saved data for weights and biases were used as initial values. At 6 s the saved data were loaded and control began at the same time. Despite the sudden change of the system, the vibration was efficiently suppressed. These results show that the present neuro-controller has effective control performance not only in simulation but also in real-time experiment even though the system is much changed abruptly.

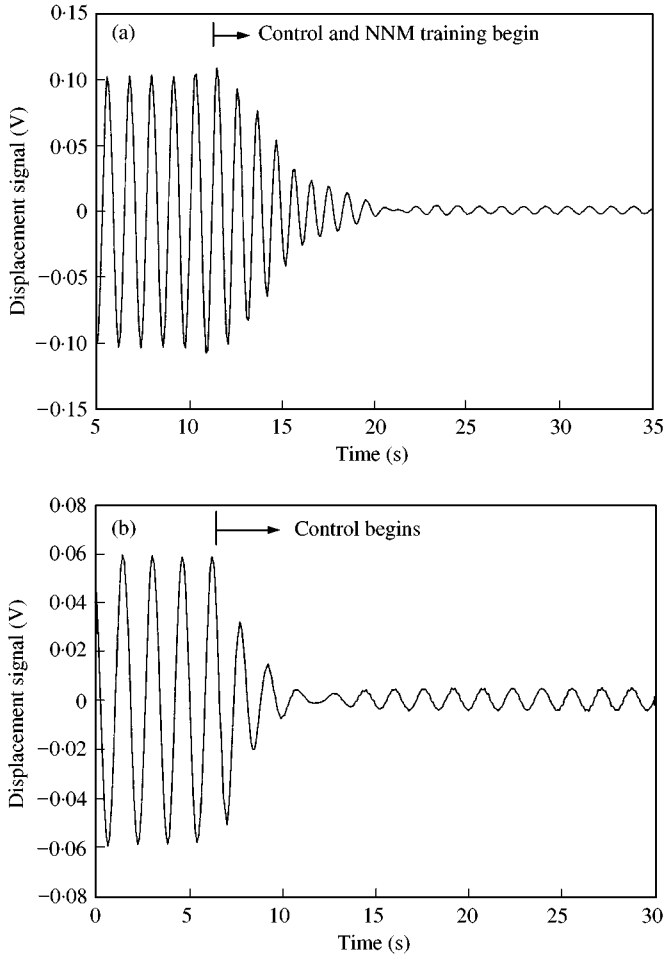

Figure 13. Adaptive vibration-control results for the Gr/epoxy $[0/90]_s$ composite specimen when 50% delamination occurs under persistent disturbance. (a) Adaptive vibration control for the 0% delaminated specimen, (b) Adaptive vibration control for the 50% delaminated specimen.

In order to highlight the adaptability of the present approach, we made comparison of the neuro-controller with a conventional linear time-invariant control. A positive position feedback (PPF) controller was designed, the transfer function of which is [23]

$$H(s)_{PPF\ filter} = K \frac{\omega_f^2}{s^2 + 2\zeta_f \omega_f s + \omega_f^2}, \tag{17}$$

where ω_f is the filter frequency, which was set to the vibration frequency of the normal specimen, and ζ_f is the filter damping ratio, which was set to 0·5 in this study. The controller gain K was adjusted to be 3 for the consideration of maximum applicable voltage. Maintaining all experimental conditions the same as those of Figure 13, we obtained controlled results with the PPF controller as shown in Figure 14. For the normal specimen we obtained a slightly degraded result because of geometric non-linearity due to large amplitudes. When the same controller was applied to the 50% delaminated specimen, we obtained very poor control effects. This fact indicates that the linear time-invariant controllers have certain performance limitations when the system parameters are changed.

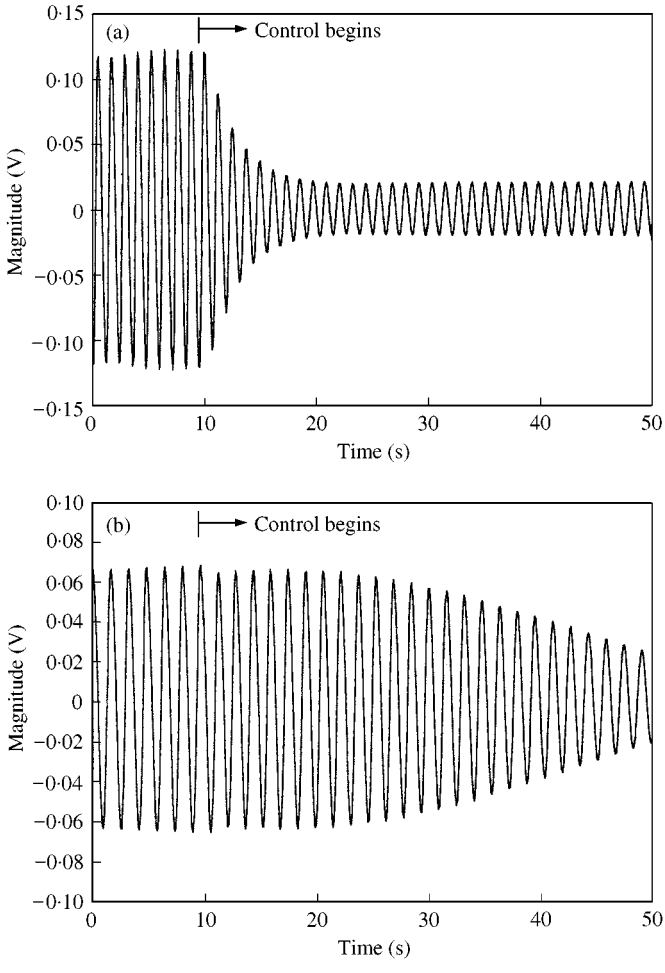

Figure 14. Vibration-control results for the Gr/epoxy $[0/90]_s$ composite specimen using the PPF controller. (a) Vibration control result for the 0% delaminated piezoactuator, (b) Vibration control result for the 50% delaminated piezoactuator.

6. SUMMARY AND CONCLUSIONS

In this paper, neuro-adaptive vibration controls of composite beams subject to sudden delamination have been investigated via both simulation and real-time control experiment. We identified the variations of the system characteristics such as natural frequencies and modal actuation forces due to delamination by the experimental modal testing. Significant reductions of vibrational levels have been observed for both numerical and real-time neuro-adaptive controls. The present neuro-adaptive controller has good robustness with respect to the system parameter variations. From these investigations the following conclusions can be drawn.

1. Variations of dynamic characteristics and actuation capabilities of composite beams have been experimentally investigated according to the subsequent delamination in the bonding layer of the piezoceramic actuator. As the delamination size increases, natural frequencies and actuation capabilities decrease significantly.

2. Numerical simulations for the adaptive vibration control have been performed. In spite of sudden changes in dynamic characteristics, the vibrations can be successfully suppressed without instability.
3. A real-time adaptive vibration-control system has been prepared using a DSP board. The present controller is proved to have good vibration suppression capabilities, even though 50% delamination occurs suddenly.
4. In this study, the real-time control has been performed to suppress only the first vibrational mode due to the limitation of hardware performance. However, it is expected that the development of hardware such as neural network chip will be accelerated. With the improvement of hardware, the present method can be extended to control multi-modal vibrations and to control the structures with higher frequencies in the near future.

ACKNOWLEDGMENTS

The present work was supported by the Korea Science and Engineering Foundation (Project No. 96-0200-05-01-3).

REFERENCES

1. M. V. GANDHI and B. S. THOMPSON 1992 *Smart Materials and Structures*, 175–191, London: Chapman & Hall.
2. T. BAILEY and J. E. HUBBARD JR. 1985 *Journal of Guidance, Control, and Dynamics* **8**, 605–611. Distributed piezoelectric polymer active vibration control of a cantilever beam.
3. S.-B. CHOI 1995 *AIAA Journal* **33**, 564–567. Alleviation of chattering in flexible beam control via piezofilm actuator and sensor.
4. M. R. BAI and G. M. LIN 1996 *Journal of Sound and Vibration* **198**, 411–427. The development of a DSP-based active small amplitude vibration control system for flexible beams by using LQG algorithms and intelligent materials.
5. J.-H. HAN, K.-H. REW and I. LEE 1997 *Smart Materials and Structures* **6**, 549–558. An experimental study of active vibration control of composite structures with a piezo-ceramic actuator and a piezo-film sensor.
6. I. E. GRADY and E. H. MEYN 1989 *Proceedings of the AIAA SDM Conference, Paper* No. 89–1411. Vibration testing of impact damaged composite laminates.
7. S. J. KIM and J. D. JONES 1996 *Journal of Intelligent Material Systems and Structures* **7**, 668–676. Effects of piezo-actuator delamination on the performance of active noise and vibration control systems.
8. B. WIDROW, R. G. WINTER and R. A. BAXTER 1988 *IEEE Transactions on Acoustics, Speech, and Signal Processing* **36**, 1109–1118. Layered neural nets for pattern recognition.
9. D. H. NGUYEN and B. WIDROW 1991 *International Journal of Control* **54**, 1439–1451. Neural networks for self-learning control systems.
10. S. D. SNYDER and N. TANAKA 1993 *Journal of Intelligent Material Systems and Structures* **4**, 373–378. A neural network for feedforward controlled smart structures.
11. S. D. SNYDER and N. TANAKA 1995 *IEEE Transactions on Neural Networks* **6**, 819–828. Active control of vibration using a neural network.
12. K. NARENDRA and K. PARTHASARATHY 1990 *IEEE Transactions on Neural Networks* **1**, 4–27. Identification and control of dynamical systems using neural networks.
13. K. KRISHNAKUMAR and L. MONTGOMERY 1992 *Smart Materials and Structures* **1**, 312–323. Adaptive neuro-control for large flexible structures.
14. V. RAO, R. DAMLE, C. TEBBE and F. KERN 1994 *Smart Materials and Structures* **3**, 354–366. The adaptive control of smart structures using neural networks.
15. K. CHANDRASHEKHARA and C. P. SMYSER 1998 *Journal of Intelligent Material Systems and Structures* **9**, 29–43. Dynamic modelling and neural control of composite shells using piezoelectric devices.

16. C. A. JENG, S. M. YANG and J. N. LIN 1997 *Journal of Intelligent Material Systems and Structures* **8**, 1035–1043. Multi-mode control of structures by using neural networks with marquardt algorithms.
17. S. M. YANG and G. S. LEE 1998 *Journal of Intelligent Material Systems and Structures* **9**, 999–1008. An optimal neural network design methodology for fast convergence and vibration suppression.
18. J.-H. HAN, K.-D. CHO, S.-H. YOUN and I. LEE 1999 *Smart Materials and Structures* **8**, 136–143. Vibration and actuation characteristics of composite structures with a bonded piezo ceramic actuator.
19. D. A. WHITE and D. A. SOFGA 1992 *Handbook of Intelligent Control*, New York: Van Nostrand Reinhold.
20. J. M. ZURADA 1992 *Introduction to Artificial Neural Systems*, 211–213, St. Paul, MN: West Publishing Company.
21. H. DEMUTH and M. BEALE 1992 *Neural Network Toolbox, for Use with MATLAB®*, Natick, MA The Math Works.
22. J. MOSCINSKI and Z. OFONOWSKI 1995 *Advanced Control with MATLAB and SIMULINK*, Chichester, UK: Ellis Horwood.
23. J.-H. HAN and I. LEE 1999 *Smart Materials and Structures* **8**, 257–267. Optimal placement of piezoelectric sensors and actuators for vibration control of a composite plate using genetic algorithms.